CrossMark

Involvement of Claudin-11 in Disruption of Blood-Brain, -Spinal Cord, and -Arachnoid Barriers in Multiple Sclerosis

Yasuo Uchida[1] · Tomohito Sumiya[1] · Masanori Tachikawa[1] · Tatsuya Yamakawa[1] · Sho Murata[1] · Yuta Yagi[1] · Kazuki Sato[1] · Alice Stephan[1] · Katsuaki Ito[1] · Sumio Ohtsuki[2] · Pierre-Olivier Couraud[3] · Takashi Suzuki[4] · Tetsuya Terasaki[1]

Abstract

It is important to understand the molecular mechanisms of barrier disruption in the central nervous system (CNS) of patients with multiple sclerosis (MS). The purpose of the present study was to clarify whether claudin-11 is involved in the disruption of two endothelial barriers (blood-brain barrier (BBB) and blood-spinal cord barrier (BSCB)) and two epithelial barriers (blood-arachnoid barrier (BAB) and blood-CSF barrier (BCSFB)) in the CNS in MS. Immunohistochemical analysis revealed that, in both normal human and mouse, claudin-11 is co-localized with claudin-5 in the brain and spinal cord capillaries. The absolute protein expression level of claudin-11 was nearly equal to that of claudin-5 in rat brain capillaries, but was 2.81-fold greater in human brain capillaries. The protein expressions of claudin-11 were significantly downregulated in the brain and spinal cord capillaries of an MS patient and experimental autoimmune encephalomyelitis (EAE) mice. Specific downregulation of claudin-11 with siRNA significantly increased the transfer of membrane-impermeable FITC-dextran across human brain capillary endothelial cell (hCMEC/D3) monolayer. As for the epithelial barrier, claudin-11 protein expression was not decreased in choroid plexus epithelial cells forming the BCSFB in EAE mice, whereas it was decreased in brain and spinal cord meninges that form the BAB. Specific downregulation of claudin-11 with siRNA in a rat choroid plexus epithelial cell (TR-CSFB) monolayer significantly increased the permeability of FITC-dextran. In conclusion, our present findings indicate that claudin-11 expression at the BBB, BSCB, and BAB, but not the BCSFB, is downregulated in multiple sclerosis, impairing the functional integrity of these barriers.

Keywords Claudin-11 · Claudin-5 · Multiple sclerosis · Blood-spinal cord barrier · Blood-arachnoid barrier · Blood-brain barrier

Abbreviations

BAB	Blood-arachnoid barrier
BBB	Blood-brain barrier
BCSFB	Blood-cerebrospinal fluid barrier
B-cap	Brain capillary
BSCB	Blood-spinal cord barrier
DDA	Data-dependent acquisition
DHT	Dihydrotestosterone
EAE	Experimental autoimmune encephalomyelitis
ER-TR7	A meningeal marker
Glut1	Glucose transporter 1
hCMEC/D3	Human cerebral microvascular endothelial cell line
LC-MS/MS	Liquid chromatography–tandem mass spectrometry
MS	Multiple sclerosis
PRM	Parallel reaction monitoring
QTAP	Quantitative targeted absolute proteomics
SC-cap	Spinal cord capillary
SRM	Selected reaction monitoring
TM-BBB	Mouse brain capillary endothelial cell line
TR-CSFB	Rat choroid plexus epithelial cell line

✉ Yasuo Uchida
yuchida@m.tohoku.ac.jp

[1] Division of Membrane Transport and Drug Targeting, Graduate School of Pharmaceutical Sciences, Tohoku University, 6-3 Aoba, Aramaki, Aoba-ku, Sendai 980-8578, Japan

[2] Faculty of Life Sciences, Kumamoto University, Kumamoto, Japan

[3] Institut Cochin, Inserm U1016, CNRS UMR8104, Paris Descartes University, Sorbonne Paris City, Paris, France

[4] Department of Pathology and Histotechnology, Tohoku University Graduate School of Medicine, Sendai, Japan

Introduction

Multiple sclerosis (MS) is an immune-mediated disorder of the central nervous system (CNS) affecting more than 2 million people worldwide, and is characterized by the invasion of autoreactive lymphocytes into the CNS and the demyelination of nerves. Current therapeutic agents/methods do not adequately suppress the pathogenesis or progression of MS. Magnetic resonance imaging has shown that CNS barrier disruption, detected by gadolinium-DTPA enhancement, occurs before the appearance of MS lesions and the development of symptoms [1], suggesting that breakdown of CNS barriers is a very early event and, indeed, could trigger MS pathogenesis. This evidence strongly supports the idea that the inhibition of CNS barrier disruption would be a rational therapeutic strategy to suppress MS pathogenesis and progression. However, the molecular mechanisms of CNS barrier disruption are not yet fully understood. Because MS often occurs in young adult women, it is considered that a hormone-dependent mechanism might be involved in the barrier disruption. Although it has been suggested that downregulation of claudin-5 at the blood-brain barrier (BBB) and claudin-3 at the blood-cerebrospinal fluid barrier (BCSFB) are involved in the impairment of barrier function in MS [2, 3], there is no evidence that claudin-5 and claudin-3 are functionally regulated by sex hormone at the CNS barriers.

Claudin-11 is a four-transmembrane protein with 207 amino acids, and is expressed in the tight junctions of myelin sheaths of CNS oligodendrocytes and Sertoli cells of testes [4, 5]. Claudin-11 is also expressed at several CNS barriers, including the BBB, BCSFB, and blood-arachnoid barrier (BAB) [6–8]. It contributes to tight-junction integrity at the blood-testis barrier, and it is upregulated by androgen [9, 10]. Notably, compared to male MS patients, more extensive CNS barrier disruption has been observed in female MS patients, especially in those with low blood testosterone levels [11]. Pre-administration of dihydrotestosterone (DHT) has alleviated the severity of experimental autoimmune encephalomyelitis (EAE) in a mouse model of MS [12]. Therefore, it is thought that loss of claudin-11 is involved in the CNS barrier disruption in MS, and the reason for the greater severity in female MS patients may be the lower level of androgen signaling. However, these ideas remain to be fully established. Furthermore, the physiological importance of claudin-11 in tight-junction formation of the CNS barriers remains uncertain.

Spinal cord capillaries form the blood-spinal cord barrier (BSCB), analogously with the BBB in brain, and its disruption is considered to allow the invasion of autoreactive lymphocytes into spinal cord parenchyma. In healthy rabbits, the transfer of impermeable markers such as [^{3}H]D-mannitol and [^{14}C]carboxyl-inulin from circulating blood into the spinal cord was greater than that into the brain [13]. The neuronal

damage and reduction in neuronal numbers in MS patients is suggested to be more significant in spinal cord than brain, because MS disability score is better correlated with atrophy of the spinal cord (especially cervical and thoracic spinal cords) than that of the brain [14]. Invasion of lymphocytes is more extensive in spinal cord than brain in acute active EAE. These findings raise the possibility that the BSCB is more likely to be impaired than the BBB in MS patients. Because the protein expression level of claudin-5 is similar in the BBB and BSCB [15], it is likely that some tight-junction protein other than claudin-5 is associated with this vulnerability of the BSCB, but it remains to be identified.

It was recently shown that lymphocytes enter the CSF from circulating blood via the leptomeninges of the spinal cord and subsequently invade spinal cord parenchyma from the CSF; this is an earlier event than direct invasion via the BSCB, and furthermore, this invasion route into CSF via the leptomeninges of spinal cord predominates over that via choroid plexus [16]. Therefore, disruption of the BAB separating the circulating blood and CSF in the leptomeninges might be a more plausible explanation than impairment of the BCSFB for lymphocyte invasion into the CSF. However, it is unknown whether the expression of claudin-11 in MS is more downregulated at the BAB than at the BCSFB. It is also unclear whether the downregulation of claudin-11 at these CNS epithelial barriers decreases the barrier integrity.

Therefore, the purpose of the present study was to clarify (1) whether claudin-11 expression is downregulated at the four CNS barriers, BBB, BSCB, BCSFB, and BAB, in MS, and (2) whether downregulation of claudin-11 expression impairs the integrity of these CNS barriers.

Materials and Methods

Materials

All materials, including probe peptides for proteomics and antibodies, are described in the supplemental data.

Animals

The animal experiments were conducted based on the ARRIVE guidelines, and the protocol was approved by the Institutional Animal Care and Use Committee at Tohoku University. For details of the animal experiments, refer to the supplemental data.

Briefly, for the induction of EAE, EAE Induction Hooke Kits (EK-2110, Hooke Laboratories, Lawrence, MA, USA) were used according to the manufacturer's instructions. EAE was induced in 11-week-old female C57BL/6J mice. Mice were immunized subcutaneously with 100-μg MOG$_{35–55}$ peptide emulsified in complete Freund's adjuvant in the neck and

lower back (0.1 mL/site, total of 0.2 mL) on day 0. Each mouse was injected intraperitoneally with 360-ng pertussis toxin at 0.1 mL/dose at 2 and at 24 h after immunization. The progression of EAE was evaluated by scoring the clinical symptoms (see Supplemental Fig. 1). Mice with a clinical score of 3.0 to 3.5 were used for experiments. The definition of clinical score was described in Supplemental Fig. 1.

Human Tissues and Cell Lines

Human normal frontal lobe sections (male, 49 years old, Caucasian; female, 60 years old, Caucasian), multiple sclerosis frontal lobe sections (male, 64 years old, Caucasian), human normal spinal cord sections (male, 59 years old, Caucasian), and multiple sclerosis spinal cord sections (male, 64 years old, Caucasian) were purchased from BioChain Institute Inc. (Newark, CA, USA) for immunohistochemistry. Frozen brain cortex of a Japanese subject (male, 77 years old) was kindly provided by Prof. Takashi Suzuki of Tohoku University Hospital and used for the analysis of absolute protein expression levels of claudin molecules. Human brain capillary endothelial cell line (hCMEC/D3 cell line) [17] was kindly provided by Dr. Pierre-Olivier Couraud (Institut Cochin, Paris, France). The research protocols used in the present study were approved by the Ethics Committees of Tohoku University School of Medicine and the Graduate School of Pharmaceutical Sciences, Tohoku University. For full details, including the other cell lines used, refer to the supplemental data.

Isolation of Human Brain Capillaries, Rat Brain, and Spinal Cord Capillaries

Human brain microvessels were isolated from the frozen brain cortex of a Japanese subject (male, 77 years old) as described previously [18]. Rat brain and spinal cord microvessels were isolated as described previously [19] with minor modifications. Details are given in the supplemental data.

Preparation of Whole-Cell Lysates and Subcellular Fractions

The whole-cell lysates and subcellular fractions from cell lines and tissues were obtained as described in the supplemental data.

Proteomics

Protein samples were digested with lysyl endopeptidase and trypsin. For shotgun proteomics, the resulting peptides were fractionated by isoelectric point-based separation into 12 fractions over a 3 to 10 linear pH range by a 3100 OFFGEL Fractionator, and the protein expression of all the claudin subtypes (claudin-1 to -27 except for claudin-13 and -21) was screened in the data-dependent acquisition (DDA) mode in a nanoLC-TripleTOF5600 (SCIEX, Framingham, MA, USA). For quantitative targeted absolute proteomics (QTAP) [20], the tryptic peptides were mixed with stable isotope-labeled peptides for the target proteins, followed by parallel or selected reaction monitoring (PRM or SRM) with an LC-MS/MS system to determine the absolute protein expression levels of the target proteins. For details, see the supplemental data.

Immunostaining

The brain tissue and backbone were excised from mice and frozen on dry ice. The cranium and dura mater were removed during excision of the brain. The frozen brain and backbone including spinal cord were sectioned with a cryostat. The tissue sections (20 μm thick) were mounted on glass slides, and fixed with cold acetone for 10 min. These sections and purchased human sections (5–10 μm in thickness, pre-fixed with acetone) were immersed in 0.2% Triton-X in PBS for 15 min followed by blocking with 10% donkey serum for 30 min at room temperature. They were immune-reacted overnight at 4 °C with the primary antibodies, then incubated with the secondary antibodies for 2 h. Nuclear staining was done with 4′,6-diamidino-2-phenylindole (DAPI) (1 μg/mL) for 10 min. Images were taken with a confocal laser scanning microscope, Leica TCS SP8 (Leica Microsystems, Wetzlar, Germany). Immunostaining of hCMEC/D3 cells treated with EAE serum and 5α-dihydrotestosterone (DHT) and HEK293 cells expressing claudin-5 and/or claudin-11 was conducted similarly. Details of the immunostaining analysis of tissue sections and cell lines are given in the supplemental data.

Western Blot Analysis

For details, see the supplemental data.

Paracellular Permeability Assay in Monolayers of hCMEC/D3 and TR-CSFB Cells Treated With Claudin siRNAs

hCMEC/D3 and TR-CSFB cells were treated with Stealth™ Selected siRNAs for human claudin-11, human claudin-5, rat claudin-11, and Negative Control Med GC Duplex (Invitrogen, Carlsbad, CA). The tight-junction integrity of monolayers of these hCMEC/D3 and TR-CSFB cells was measured by means of paracellular permeability assay using 70 kDa FITC-dextran, a cellular membrane-impermeable substance. The effect of siRNA treatment on the protein expression levels of target molecules was quantified by means of western blot analysis. The contributions of claudin-11 and

a

b

c
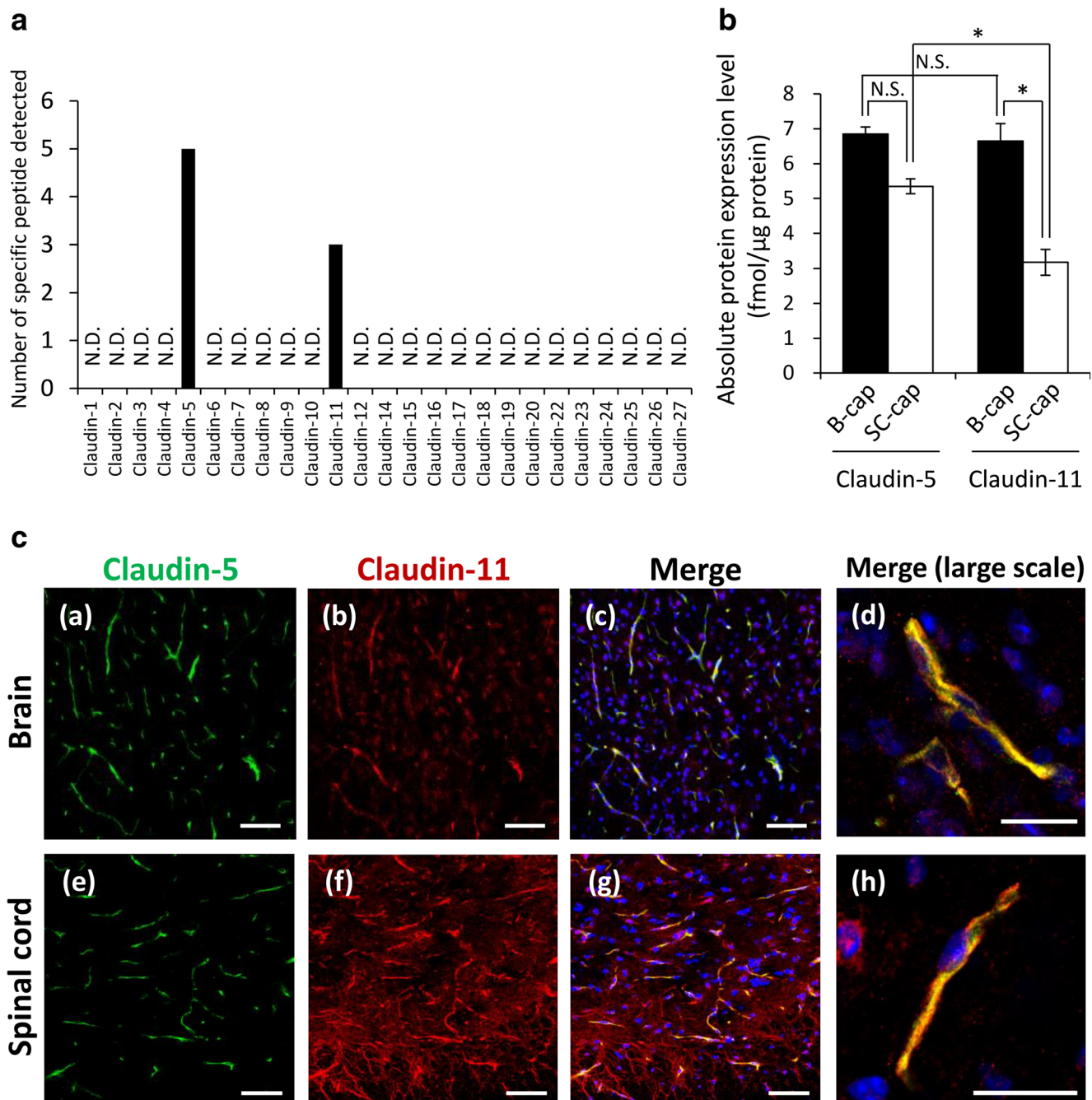
claudin-5 to the tight-junction formation were calculated as described in the supplemental data.

Statistical Analysis

An unpaired, two-tailed Student's *t* test was performed to determine the statistical significance of differences between two groups. For more than two groups, one-way analysis of variance (ANOVA) followed by Dunnett's *t* test or Bonferroni's test (as indicated in the table and figure legends) was employed. The standard error of the mean (SEM) was

calculated according to the law of propagation of error as described previously [21].

Results

Protein Expression of Claudin-11 in Normal Rodent Blood-Brain Barrier and Blood-Spinal Cord Barrier

To assess the importance of claudin-11 among the claudin family members in rat, especially compared with claudin-5,

◀ **Fig. 1** Protein expression of claudin-11 in normal rodent blood-brain barrier and blood-spinal cord barrier. **a** Pooled rat brain capillaries were isolated from the frozen brains of three normal Wistar rats. Whole-tissue lysate (1 mg protein/sample) was digested with Lys-C and trypsin, and the digests were separated into 12 fractions by off-gel electrophoresis. Each fraction was examined with the nanoLC-TripleTOF5600 in the data-dependent acquisition (DDA) mode. The obtained data was analyzed with Protein Pilot software (Sciex), and searched against the rat UniProt database, which includes the amino acid sequences of claudin-1 to -27, except for claudin-13 and -21. The names of claudin-26 and -27 in the UniProt database are "transmembrane protein 114" and "transmembrane protein 235," respectively. Peptides with a "confidence value" of more than 0.99 in the Protein Pilot search were defined as reliably identified, and were selected. Whether peptides were unique (specific) to a single protein among the rat proteome was checked by NCBI protein blast search. The numbers of reliably detected peptides specific for individual claudin subtypes are shown in this figure. Their peptide sequences are listed in Supplemental Table 1. *N.D.* not detected. **b** Whole-tissue lysates of the pooled rat brain (B-cap) and spinal cord (SC-cap) capillaries were prepared from 3 normal frozen brains and 12 normal frozen spinal cords (Wistar rat), respectively. The whole-tissue lysates (50 μg protein/sample) were digested with Lys-C and trypsin. Using peptide samples spiked with internal standard peptides, the absolute protein expression levels of claudin-11 and -5 were measured by the nanoLC-TripleTOF5600 in the PRM/MRM-HR mode (two injections/sample). The protein expression level of each molecule was calculated from the quantitative data obtained from four sets of transitions. The data represent the mean ± SEM. These data were analyzed statistically by means of one-way analysis of variance (ANOVA) and Bonferroni's test. *$p < 0.01$, significantly different. *N.S.* not significantly different ($p > 0.01$). **c** Brain and backbone (containing the spinal cord) excised from normal C57BL/6J mice were frozen with dry ice and sliced into 20-μm sections with a cryostat. The slices were fixed with cold acetone and co-stained with anti-claudin-5 (green; *a, e, c, d, g, h*) and anti-claudin-11 (red; *b, f, c, d, g, h*) antibodies. Nuclei were stained with DAPI (blue in merged images; *c, d, g, h*). Scale bar, 75 μm (*a, b, c, e, f, g*) or 25 μm (*d, h*)

which is responsible for the tight junctions at the BBB, we performed LC-MS/MS-based comprehensive proteomic analysis and quantitative targeted absolute proteomic (QTAP) analysis. Three peptides specific for claudin-11 and five peptides specific for claudin-5 were detected with high reliability, while no peptides specific for other claudin subtypes were detected (Fig. 1a and Supplemental Table 1). The absolute protein expression levels of claudin-11 and claudin-5 were almost equal in the whole-cell lysate of isolated rat brain capillaries (Fig. 1b; claudin-11, 6.65 fmol/μg protein; claudin-5, 6.85 fmol/μg protein; $p > 0.01$, Bonferroni's test). However, the protein expression level of claudin-11 in the whole-cell lysate of the isolated rat spinal cord capillaries was significantly smaller than that of claudin-5 (claudin-11, 3.18 fmol/μg protein; claudin-5, 5.35 fmol/μg protein; $p < 0.01$, Bonferroni's test), and was also 2.09-fold smaller than that of claudin-11 in the brain capillaries (Fig. 1b; $p < 0.01$, Bonferroni's test).

To understand whether claudin-11 and claudin-5 are expressed and function in the same or different capillary endothelial cells, the localization of both proteins in the brain and spinal cord was examined by immunohistochemical

analysis. Because claudin-11 has been reported to be expressed in oligodendrocytes of mouse spinal cord and in plasma membranes (cell junctions) of Sertoli cells in testis [4, 5], we first confirmed the reactivity of claudin-11 antibody used in the present study (Supplemental Fig. 2). In both brain and spinal cord sections of normal mouse, the signals of claudin-5 (a marker protein specifically expressed in capillary endothelial cells) overlapped with those of claudin-11 in almost all capillary endothelial cells (Fig. 1c). The red-colored signals in the merged pictures (Fig. 1c (*c, g*)) represent the expression of claudin-11 in oligodendrocytes. Furthermore, claudin-11 protein was clearly detected in the plasma membrane fraction of a mouse brain capillary endothelial cell line (TM-BBB4) and very slightly detected in the cytosol fraction (Supplemental Fig. 3). The band intensity calculated with ImageJ software for the cytosol fraction was 12.1% of the plasma membrane fraction. These results support the idea that claudin-11 is localized at the plasma membrane of capillary endothelial cells.

Protein Expression Analysis of Claudin-11 in Normal Human Blood-Brain Barrier, Blood-Spinal Cord Barrier, and a Human Brain Capillary Endothelial Cell Line (hCMEC/D3)

The absolute protein expression level of claudin-11 in whole-cell lysate of brain capillaries isolated from human normal brain was 18.4 fmol/μg protein, which is 2.81-fold greater than that of claudin-5 (6.56 fmol/μg protein) (Fig. 2a; $p < 0.05$, t test). hCMEC/D3 cells showed a single band corresponding to the molecular weight of claudin-11 protein in western blotting, while claudin-11 was not detected in HEK293 cells, which are claudin-11-negative (Fig. 2b). hCMEC/D3 cells also showed a 1.49-fold greater protein expression level of claudin-11 than claudin-5 in the plasma membrane fraction (Fig. 2c; claudin-11, 3.31 fmol/μg protein; claudin-5, 2.22 fmol/μg protein; $p < 0.05$, t test). Immunohistochemical analysis showed that the signals of claudin-11 in human brain (male 49 years old, female 60 years old) and spinal cord sections overlapped with those of claudin-5 (Fig. 2d), as was also the case in mouse sections, suggesting that claudin-11 is co-expressed in the same capillary endothelial cells as claudin-5. Interestingly, in contrast to the situation in mouse, claudin-11 signals on oligodendrocytes were negligible, suggesting that claudin-11 is mainly expressed in the capillaries of human brain and spinal cord.

Downregulation of Claudin-11 Protein in Brain and Spinal Cord Capillaries of EAE Mice and a MS Patient

To clarify whether claudin-11 expression level is decreased at the BBB and BSCB in MS, brain and spinal cord sections of
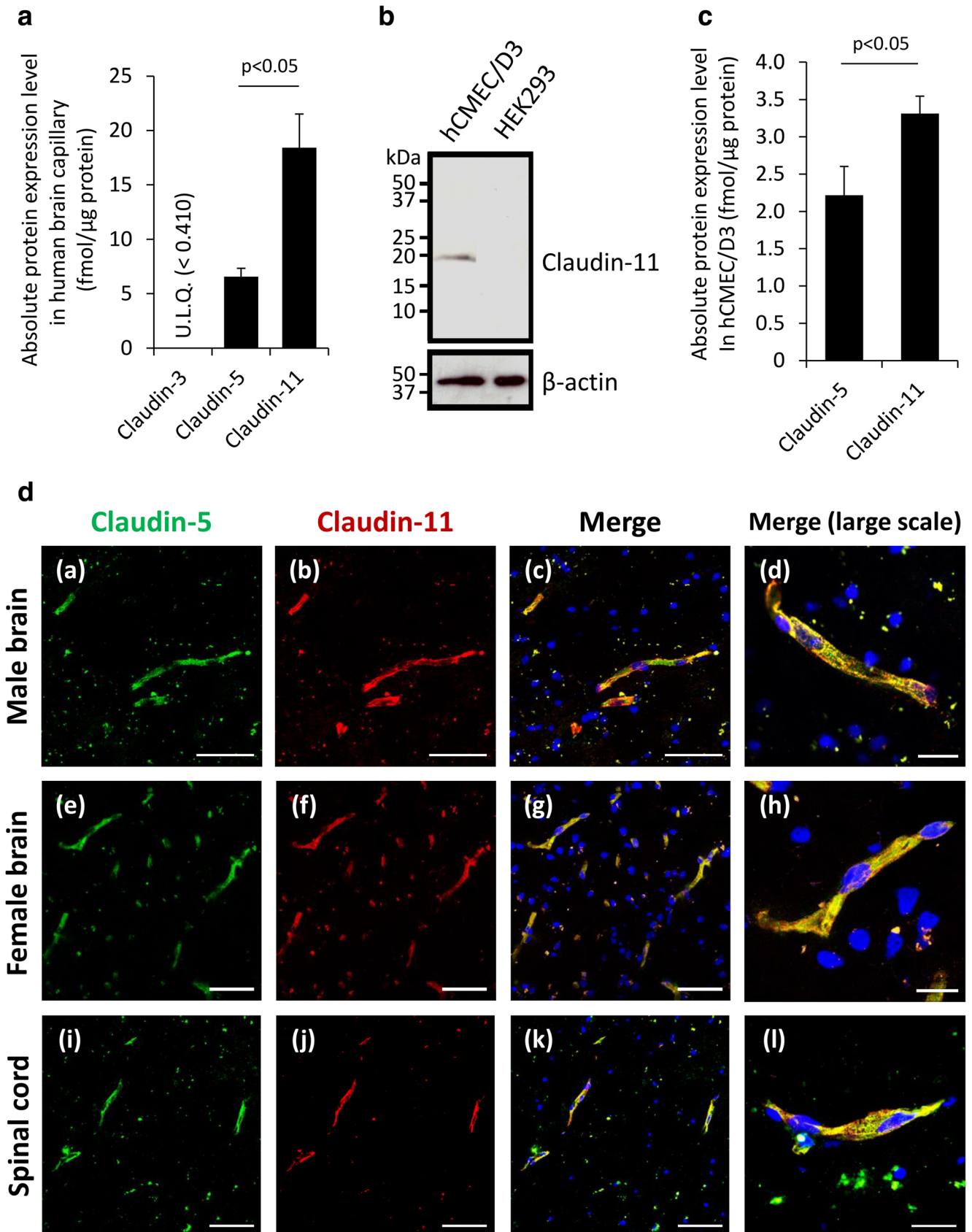
Fig. 2 Protein expression of claudin-11 in normal human blood-brain barrier, blood-spinal cord barrier, and a human brain capillary endothelial cell line (hCMEC/D3 cell). **a** Whole-tissue lysate of human brain capillaries isolated from frozen normal brain cortex (77 years old, male) was digested with Lys-C and trypsin. The peptide samples spiked with internal standard peptides were measured by the nanoLC-4000QTRAP in the SRM mode using three or four sets of SRM transitions per peptide pair (non-labeled target peptide and the corresponding stable-isotope-labeled internal standard peptide). The data represent the mean ± SEM. $p < 0.05$, significantly different between two groups (Student's t test). Claudin-3 was not detected and so the protein expression level was estimated to be under the limit of quantification (ULQ; < 0.410 fmol/μg protein). **b** Whole-cell lysates prepared from hCMEC/D3 cells and HEK293 cells (as a claudin-11-negative cell line) were subjected to SDS-PAGE. Western blot analysis was performed with anti-claudin-11 and anti-β-actin antibodies. Molecular mass in kilo Daltons is shown on the left. The bands at 19 and 42 kDa correspond to the molecular weights of claudin-11 and β-actin, respectively. **c** The plasma membrane fraction of hCMEC/D3 cells was digested with Lys-C and trypsin, and the protein expression levels of claudin-11 and -5 were quantified by means of HPLC-API5000 according to the same procedure as used for the human brain capillary sample. The data represent the mean ± SEM. $p < 0.05$, significantly different between two groups (Student's t test). **d** Human normal frontal lobe sections from a male donor (49 years old, Caucasian) and a female donor (60 years old, Caucasian) and human normal spinal cord sections from a male donor (59 years old, Caucasian) were purchased from BioChain Institute Inc. The slices were co-stained with antibodies against claudin-5 (green; *a, e, i, c, d, g, h, k, l*) and claudin-11 (red; *b, f, j, c, d, g, h, k, l*). Nuclei were stained by DAPI (blue in merged images; *c, d, g, h, k, l*). Scale bar, 75 μm (*a, b, c, e, f, g, i, j, k*) or 25 μm (*d, h, l*)

EAE mice (clinical score, 3.0 to 3.5; Supplemental Fig. 1) were stained with anti-claudin-11 antibody together with antibody to glut1, which is specifically expressed in capillary endothelial cells at the same level in normal and EAE mice [22] (Fig. 3 for high magnification and Supplemental Fig. 4 for low magnification). The claudin-11 signals were significantly decreased in the capillaries of brain and spinal cords in EAE mice, compared to normal mice (Fig. 3a, b). Low-magnification pictures showed that the claudin-11 signals were decreased in a broad range of capillaries (Supplemental Fig. 4a, b), and the signal intensity ratio (claudin-11/glut1) was significantly decreased by 30.8 and 41.1% in the brain and spinal cord capillaries, respectively, of the EAE mice (Fig. 3c; $p < 0.05$, t test). We utilized these changes together with the absolute protein expression levels of claudin-11 in the normal isolated brain and spinal cord capillaries (Fig. 1b) to estimate the absolute protein expression levels of claudin-11 in the EAE mice. The level in the spinal cord was 1.87 fmol/μg protein, and was significantly smaller than that (4.60 fmol/μg protein) in the brain capillaries (Fig. 3d; $p < 0.05$, t test). The claudin-11 signals in the capillaries in sections of brain frontal lobe and spinal cord of the MS patient were also decreased compared with normal tissues (Fig. 3e, g). Decreased claudin-11 signals relative to glut1 signals were also observed in the low-magnification pictures (Supplemental Fig. 4c, d). The signal intensity ratio (claudin-11/glut1) was significantly
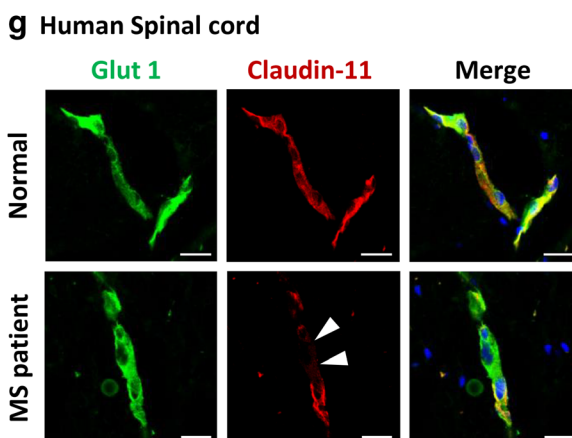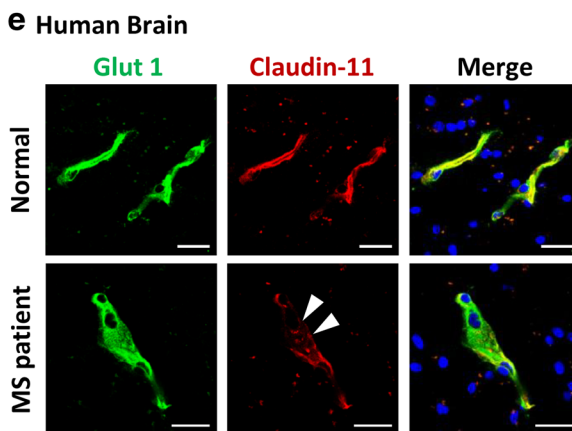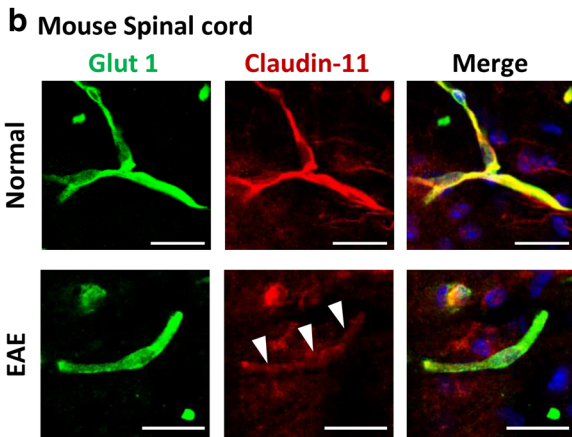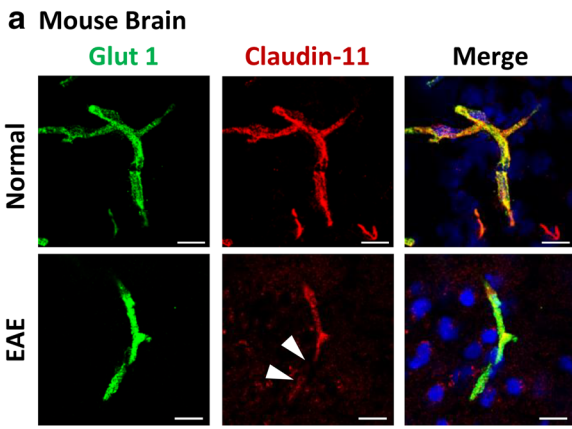
decreased by 39.4 and 48.4% in the brain and spinal cord capillaries, respectively, of the MS patient (Fig. 3f, h; $p < 0.05$, t test).

Dihydrotestosterone Suppresses the Decrease in Claudin-11 Protein Expression at the Plasma Membrane of EAE-Serum-Treated hCMEC/D3 Cells
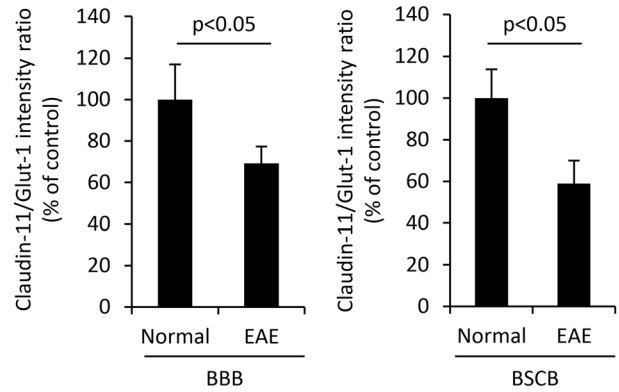
It has been reported that androgen suppresses CNS barrier disruption in MS patients [11]. It has also been reported that the tight-junction-forming ability of claudin-11 is enhanced by androgen at the blood-testis barrier [10], though it is not clear whether claudin-11 at the CNS barrier is regulated by androgen. To understand whether claudin-11 is involved in the androgen-induced suppression of BBB and BSCB disruption in MS, EAE-serum-treated hCMEC/D3 cells (considered to be a multiple sclerosis BBB model) were exposed to dihydrotestosterone (DHT), and changes in the expression of claudin-11 were examined (Fig. 4a). The signals of claudin-11 disappeared on the plasma membrane of EAE-serum-treated hCMEC/D3 cells and appeared in the cytosol of some of the cells. The loss of claudin-11 from the plasma membrane was suppressed by DHT treatment. Furthermore, the plasma membrane fraction was isolated by the Minute Plasma Membrane Protein Isolation Kit (Invent Biotechnologies, Plymouth, MN, USA) and used for the absolute quantification of claudin-11. The protein expression level of claudin-11 was 0.312 ± 0.021 fmol/μg protein (mean ± SEM) in the plasma membrane fraction of EAE-serum-treated hCMEC/D3 cells, and significantly smaller ($p < 0.01$, Bonferroni's test) than that of normal serum-treated cells (1.51 ± 0.11 fmol/μg protein). In the plasma membrane fraction of the DHT- plus EAE-serum-treated hCMEC/D3 cells, it was 1.12 ± 0.12 fmol/μg protein ($p < 0.01$, significantly different from that of EAE-serum-treated hCMEC/D3 cells, Bonferroni's test).

Contributions of Claudin-11 and Claudin-5 to Tight-Junction Formation in Human Brain Capillary Endothelial Cells

To clarify whether the downregulation of claudin-11 protein expression at the BBB and BSCB of MS contributes to the decrease in the barrier integrity, we measured the permeability of dextran (70 kDa) across a monolayer of claudin-11-knockdown hCMEC/D3 cells (Fig. 4b, c). We confirmed that claudin-11 siRNA treatment caused a significant decrease in the protein expression level of claudin-11 ($p < 0.05$, Dunnett's test); claudin-5 expression was also decreased, though without statistical significance ($p > 0.05$, Dunnett's test). The dextran permeability was significantly increased ($p < 0.01$, Dunnett's test), suggesting that downregulation of claudin-11 expression contributes to the decrease of barrier integrity. hCMEC/D3 cells treated with claudin-5 siRNA also showed significantly
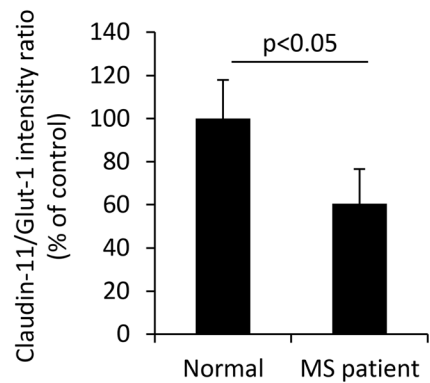
a Mouse Brain
Glut 1 / Claudin-11 / Merge (Normal, EAE)

b Mouse Spinal cord
Glut 1 / Claudin-11 / Merge (Normal, EAE)

c Decreased level of claudin-11 signal in EAE mice

d Absolute abundance of claudin-11 in EAE mice

e Human Brain
Glut 1 / Claudin-11 / Merge (Normal, MS patient)
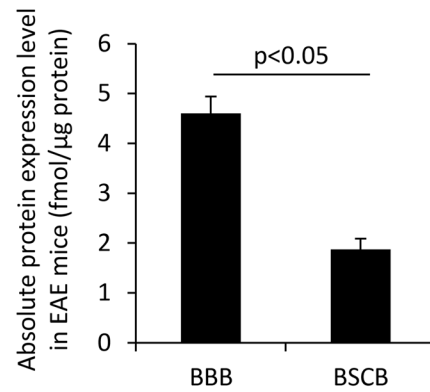
f Decreased level of claudin-11 signal at the BBB in MS

g Human Spinal cord
Glut 1 / Claudin-11 / Merge (Normal, MS patient)

h Decreased level of claudin-11 signal at the BSCB in MS
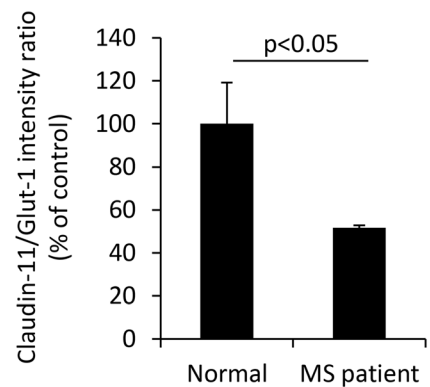
Fig. 3 Downregulation of claudin-11 protein in the brain and spinal cord capillaries of EAE mice and an MS patient. **a**, **b** EAE was induced in female C57BL/6J mice by immunization with MOG$_{35-55}$ peptide emulsified in complete Freund's adjuvant. Mice also received intraperitoneal injections of 360-ng pertussis toxin in 100 μL PBS at 2 and 24 h after MOG injection. In control mice, PBS was injected instead of MOG emulsion and pertussis toxin. EAE mice with a clinical score of 3 to 3.5 were used for immunohistochemistry. Brain and backbone (including the spinal cord) excised from control (normal) and EAE mice were frozen with dry ice and sliced into 20-μm sections with a cryostat. The slices were fixed with cold acetone and co-stained with the antibodies against glut1 (green) and claudin-11 (red). Nuclei were stained with DAPI (blue in merged images). Scale bar, 25 μm. Arrowheads indicate the loss of claudin-11 signal in the capillaries. **c** The fluorescence intensities of glut1 and claudin-11 in three capillaries in the mouse brain and spinal cord sections were quantified by LAS X software. The intensity ratio (claudin-11/glut1) was calculated and compared between normal (control) and EAE mice. The value of normal mice was normalized to 100%. The data represent the mean ± SD. **d** The absolute protein expression level of claudin-11 at the BBB and BSCB in EAE mice was estimated by the multiplication of [absolute protein expression level of claudin-11 at BBB and BSCB in normal rat] (Fig. 1b) and [100 − (%decrease in claudin-11/glut1 intensity ratio in EAE mice)] (**c**). The protein expression level in normal rats was assumed to be the same as that in normal mice. The data represent the mean ± SEM. The SEM was calculated according to the law of propagation of error. **e**, **g** Human normal frontal lobe section (male, 49 years old, Caucasian), MS frontal lobe section (male, 64 years old, Caucasian), normal spinal cord section (male, 59 years old, Caucasian), and MS spinal cord section (male, 64 years old, Caucasian) were purchased from BioChain Institute Inc. The slices were co-stained with antibodies against glut1 (green) and claudin-11 (red). Nuclei were stained with DAPI (blue in merged images). Scale bar, 25 μm. Arrowheads indicate the loss of claudin-11 signal in the capillaries. **f**, **h** The fluorescence intensities of glut1 and claudin-11 in three capillaries in the human brain and spinal cord sections were quantified by LAS X software. The intensity ratio (claudin-11/glut1) was calculated and compared between normal and MS sections. The value of normal sections was normalized to 100%. The data represent the mean ± SD

increased dextran permeability ($p < 0.01$, Dunnett's test), but these cells showed significant decreases in protein expression of not only claudin-5 but also claudin-11 ($p < 0.05$, Dunnett's test). Additional experiment to check the off-target effect for the other potential BBB components was conducted with the claudin-11-knockdown hCMEC/D3 cells by a relative quantitative proteomic analysis, and then, no significant change was observed in the protein expression level of occludin, VE-cadherin, and glucose transporter 1 between knockdown and control cells ($p > 0.05$, Bonferroni's test).

Next, the contributions of claudin-11 and claudin-5 to tight-junction formation were calculated as described in the "Materials and Methods" section. As shown in Table 1, the contribution (total activity) of claudin-11 was 2.03-fold smaller than that of claudin-5 in the hCMEC/D3 cell monolayer (6.59 for claudin-11, 13.4 for claudin-5 ($\times 10^{-6}$ cm/min)). To evaluate the contributions at the human BBB in vivo, the activity per 1 mol of claudin-11 or claudin-5 in the hCMEC/D3 cell monolayer (single-molecule activity) was combined with the absolute protein expression level in isolated human brain capillaries. The contributions of claudin-11 and claudin-5 to tight-junction formation at the human in vivo BBB were estimated to be almost equal (36.7 for claudin-11, 39.6 for claudin-5).

Cis and Trans Binding Patterns of Claudin-11 and Claudin-5 in Tight-Junction Formation

The knockdown of claudin-5 expression by siRNA also caused downregulation of claudin-11 expression in hCMEC/D3 cells (Fig. 4b). In order to understand the molecular mechanism underlying this observation, the interaction patterns of claudin-11 and claudin-5 were investigated using gene-transfected HEK293 cell lines (Fig. 5). We considered that, if the signals of claudin proteins are observed on the plasma membrane at locations where there is no neighboring cell, the claudin proteins would be stabilized on the plasma membrane by cis-binding. On the other hand, if the signals are observed at cell-cell junctions, the claudin proteins would be stabilized on the plasma membrane by trans-binding. As shown in Fig. 5a, in a monoculture of claudin-11-transfected cells, the green signals of claudin-11 were observed at cell-cell junctions, but were not observed at plasma membrane locations where there is no neighboring cell. On the other hand, in a monoculture of claudin-5-transfected cells, signals of claudin-5 were observed at both locations (Fig. 5b). In a co-culture of claudin-11- and claudin-5-transfected cells, the cell-cell junctions showed claudin-5 signals but no claudin-11 signal (Fig. 5c). This suggests that claudin-5 and claudin-11 do not exhibit trans-binding to each other. In claudin-5 and claudin-11 double-transfected cells, the yellow signals of overlapping claudin proteins were observed at both plasma membrane locations where there are neighboring cells and where there are no neighboring cells (Fig. 5d). These results suggest that the binding patterns of claudin-11 and claudin-5 in cells expressing both of them would follow one of the two models illustrated in Fig. 5e.

Protein Expression of Claudin-11 at the Epithelial Barriers of the Central Nervous System in EAE Mouse and Its Contribution to Epithelial Tight-Junction Formation

Invasion of lymphocytes into the CSF is observed in MS, indicating that not only the capillary endothelial cell barriers but also the epithelial barriers (BCSFB (choroid plexus) and BAB) are disrupted. Therefore, we histochemically examined the expression of claudin-11 in the choroid plexus of EAE mice, together with the expression of claudin-3, which has been reported to contribute to tight-junction formation of the BCSFB [3]. The signals of claudin-11 and claudin-3 were observed in the plasma membrane of choroid plexus epithelial cells of both EAE and normal mice (Fig. 6a). Western blot
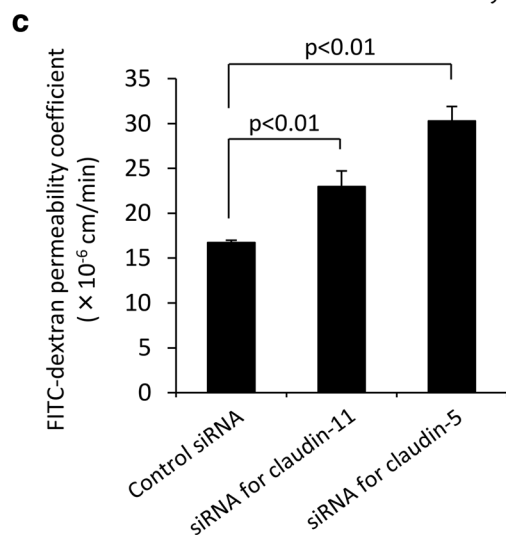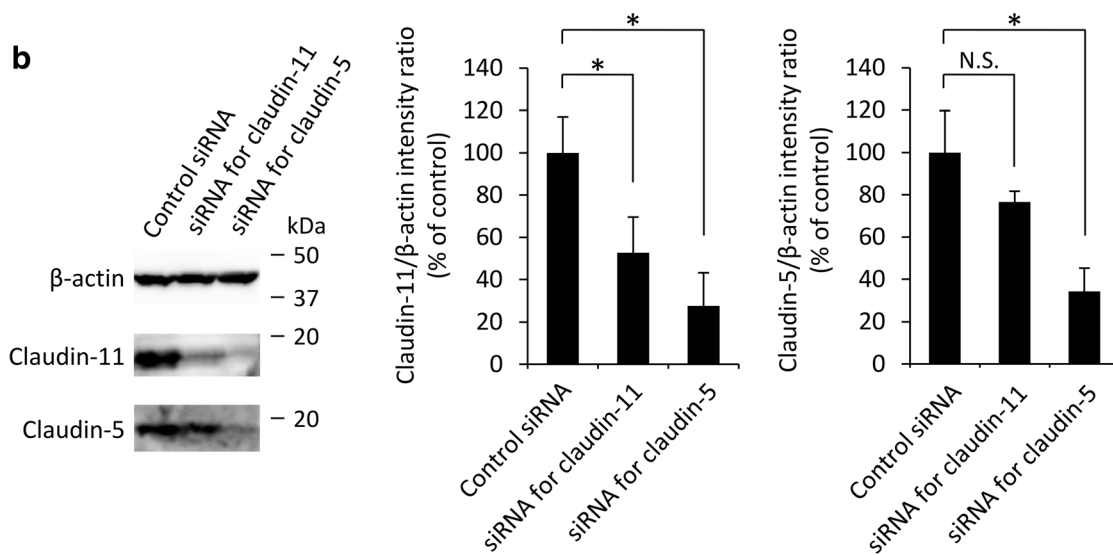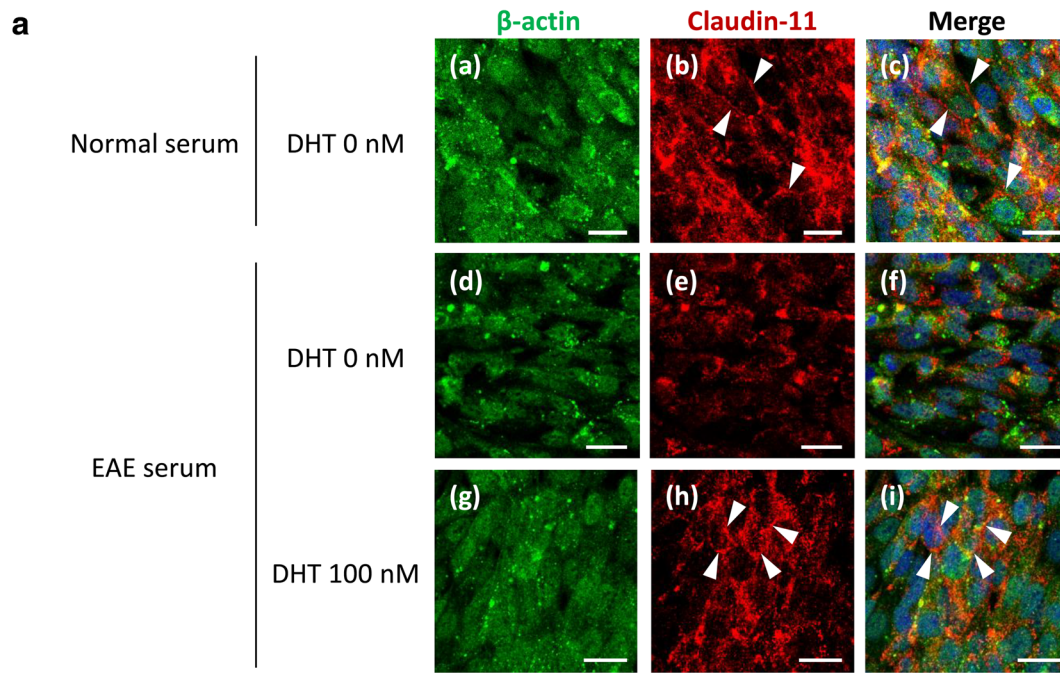
◄ **Fig. 4** Effect of androgen on claudin-11 protein expression in EAE-serum-treated hCMEC/D3 cells, and the influence of claudin-11 downregulation on barrier integrity of a hCMEC/D3 cell monolayer. **a** hCMEC/D3 cells were cultured in normal medium with or without dihydrotestosterone (DHT; 100 nM) for 5 days. After that, the medium was changed to medium containing 10% serum collected from normal or EAE mice (clinical score > 3.0), and incubation was continued with or without dihydrotestosterone (100 nM) for 24 h. The cells were fixed with 4% PFA/phosphate buffer and co-stained with the antibodies against β-actin (green; *a, d, g, c, f, i*) and claudin-11 (red; *b, e, h, c, f, i*). Nuclei were stained with DAPI (blue in merged images; *c, f, i*). Scale bar, 25 μm. Arrowheads indicate the expression of claudin-11 in the cell membrane. **b** hCMEC/D3 cells were treated with 20 nM siRNA for 6 h and cultured in medium without siRNA for 18 h. After 7 days, whole-cell lysate (22.5 μg) of hCMEC/D3 cells was prepared and subjected to SDS-PAGE, and western blot analysis was performed with anti-claudin-11, anti-claudin-5, and anti-β-actin antibodies. Molecular mass in kilo Daltons is shown on the *right*. The band intensities were calculated with ImageJ software and those of claudin-11 and claudin-5 were normalized with respect to β-actin. The band intensity ratio (claudin-11/β-actin, or claudin-5/β-actin) in the control siRNA condition was normalized to 100%. *N.S.* not significantly different from the control siRNA ($p > 0.05$). *$p < 0.05$, significantly different from the control siRNA, based on one-way analysis of variance (ANOVA) followed by Dunnett's test. The data represent the mean ± SD ($n = 3$). **c** hCMEC/D3 cells were treated with siRNA and cultured in 6-well Transwell plates for 7 days under the same experimental conditions as used for the western blot experiment, and then were used for FITC-dextran permeability analysis. After removal of the medium, 1 mg/mL FITC-dextran (70 kDa) solution (1.5 mL) was added to the Transwell insert. The concentration of FITC-dextran in the receiver well was measured at 15, 30, and 45 min. The permeability coefficient was calculated as described in the "Materials and Methods" section. $p < 0.01$, significantly different from the control siRNA condition, based on one-way analysis of variance (ANOVA) followed by Dunnett's test. The data represent the mean ± SD ($n = 3$)

analysis showed that the band intensities of both claudins in the choroid plexus were almost identical in EAE and normal mice (Fig. 6b; the claudin-11/β-actin and claudin-3/β-actin band intensity ratios in EAE mice were 92.3 and 89.1% of normal mice, respectively). By contrast, at the brain surface (meninges), the claudin-11 signal overlapped with that of ER-TR7, which is a marker of arachnoid and pia mater, in normal mice, while the claudin-11 signal disappeared in the meninges of EAE mice (Fig. 6c). In the meninges of the upper thoracic spinal cord, the claudin-11 signal was observed as a thin line on the meninges layer stained with ER-TR7 antibody (dura, arachnoid, and pia mater) in normal mice, but was greatly decreased in the ER-TR7 antibody-stained meninges layer in EAE mice (Fig. 6d). Furthermore, the claudin-11 signal was also greatly decreased in the ER-TR7 antibody-stained meninges layer of the lower thoracic spinal cord in EAE mice (Supplemental Fig. 5e, f, arrow). Many invading cells were observed in the parenchyma of the spinal cord in EAE mice (Fig. 6d (*f*), arrow; blue-colored nuclei), but not in normal mice. The invasion sites (blue-colored nuclei) appeared to be close to meninges where the signal of claudin-11 was relatively weak (Supplemental Fig. 5e, f, arrow). The nuclear staining

(blue) in the spinal cord parenchyma overlapped with the signals of CD3e (Supplemental Fig. 6), suggesting that the invading cells were CD3-positive T lymphocytes from the circulating blood.

We next investigated whether downregulation of claudin-11 expression at the CNS epithelial barrier decreases the barrier integrity by using a rat choroid plexus epithelial cell line (TR-CSFB). Claudin-11 siRNA treatment reduced the protein expression of claudin-11 (Fig. 6f; the claudin-11/Na⁺/K⁺-ATPase band intensity ratio was 58.0% of control siRNA group; $p < 0.05$, t test), and increased dextran permeability across the TR-CSFB cell monolayer (Fig. 6g; 96.8×10^{-6} cm/min for claudin-11 siRNA group and 72.8×10^{-6} cm/min for control siRNA group; $p < 0.05$, t test). These results suggest that the downregulation of claudin-11 expression increases the paracellular permeability in the CNS epithelial barrier.

Discussion

The present study has provided the first evidence that claudin-11 contributes to tight-junction formation in the CNS endothelial and epithelial barriers, and its protein expression level is significantly downregulated at the BBB, BSCB, and BAB in MS. Claudin-11 and claudin-5 appeared to contribute equally to tight-junction formation at the BBB (Table 1), whereas the absolute protein expression level of claudin-11 was significantly smaller than that of claudin-5 at the BSCB (Fig. 1b) and became extremely small in EAE mice (Fig. 3d). T lymphocyte invasion into spinal cord parenchyma was observed at regions where claudin-11 expression was decreased at the BAB in EAE mice (Fig. 6d and Supplemental Figs. 5 and 6). These results suggest that downregulation of claudin-11 expression at the BSCB and spinal cord BAB facilitates the invasion of autoreactive lymphocytes into the spinal cord parenchyma in MS; this would be consistent with a report that the neuronal damage in the spinal cord is greater than that in the brain in MS [14].

Until now, claudin-11 had not been considered to play an important role at the BBB and BSCB, because its messenger RNA (mRNA) expression is relatively small compared to other claudin subtypes, such as claudin-5, -10, and -22 [23]. However, protein expression level generally reflects molecular function better than the mRNA expression level, so we conducted a comprehensive proteomic analysis using isolated rat brain capillaries, and detected claudin-11 protein in addition to claudin-5 (Fig. 1a). The possibility that claudin-11 protein in the isolated capillary fraction is due to contamination with oligodendrocytes was ruled out by the observation that claudin-11 was expressed in human and mouse brain capillary endothelial cell lines (hCMEC/D3 and TM-BBB4 cells, respectively) (Fig. 2 and Supplemental Fig. 3), as well as by

Table 1 Contributions of claudin-11 and claudin-5 to tight-junction formation at the human blood-brain barrier

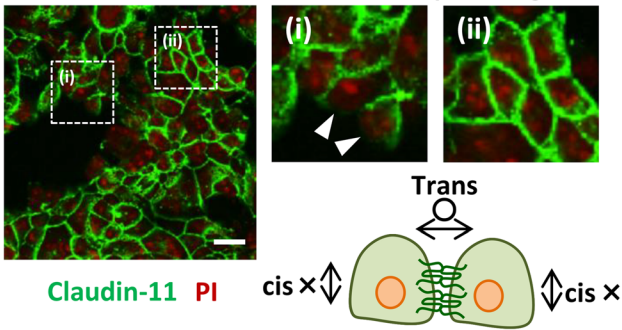|		Claudin-11	Claudin-5
Difference in FITC-dextran permeability coefficient [claudin siRNA-control siRNA] ($\times 10^{-6}$ cm/min)		6.25 ± 0.72	13.5 ± 0.7
Knockdown efficiency (%)	siRNA for claudin-11	47.4 ± 9.8	23.4 ± 8.3
	siRNA for claudin-5	72.3 ± 9.4	65.6 ± 9.2
Absolute protein expression level in hCMEC/D3 (fmol/μg protein)		3.31 ± 0.23	2.22 ± 0.38
Single-molecule activity (($\times 10^{-6}$ cm μg protein)/(min·fmol)) [= contribution of 1 mol of claudin to the change of FITC-dextran permeability coefficient]		1.99 ± 0.86	6.04 ± 1.62
Total activity in hCMEC/D3 ($\times 10^{-6}$ cm/min) [= contribution of each claudin to the restriction of FITC-dextran permeability in hCMEC/D3 cell monolayer]		6.59 ± 2.98	13.4 ± 3.9
Absolute protein expression level in human brain capillary (fmol/μg protein)		18.4 ± 3.1	6.56 ± 0.77
Activity at the human blood-brain barrier ($\times 10^{-6}$ cm/min) [= contribution of each claudin to the restriction of FITC-dextran permeability in human blood-brain barrier]		36.7 ± 15.3	39.6 ± 10.3

Difference in FITC-dextran permeability coefficient in an hCMEC/D3 cell monolayer [(claudin-11 or claudin-5 siRNA condition) − (control siRNA condition)] was calculated from the results in Fig. 4c. The knockdown efficiency of claudin-11 and -5 proteins in hCMEC/D3 cell monolayer by the respective siRNA was calculated from the data in Fig. 4b. Absolute protein expression levels in hCMEC/D3 cells and human brain capillaries were taken from the data in Fig. 2a, c, respectively. Single-molecule activity is the contribution per one claudin-11 or − 5 molecule to the change of the FITC-dextran permeability coefficient, and was calculated as described in the "Materials and Methods" section. Total activity (= contribution to tight-junction formation) in an hCMEC/D3 monolayer and in human blood-brain barrier was calculated by multiplying the [single molecule activity] and the [absolute protein expression level in hCMEC/D3 cells] or [absolute protein expression level in human brain capillaries], respectively. Each value represents the mean ± SEM. The SEM was calculated according to the law of propagation of error

the observation of claudin-11 signals in the capillaries in brain and spinal cord sections (Figs. 1c and 2d). Thus, we can conclude that claudin-11 is expressed in the capillary endothelial cells of brain and spinal cord.

Interestingly, the absolute protein expression levels of claudin-5 and -11 in brain capillaries were almost equal in rat (Fig. 1b), whereas human brain capillaries and hCMEC/D3 cells exhibited more abundant protein expression of claudin-11 than claudin-5 (Fig. 2a, c). There is no species difference in the protein expression level of claudin-5 between rat and human, whereas claudin-11 is 2.77-fold more abundantly expressed in human than rat (Figs. 1b and 2a). Although it is not feasible to completely remove other parenchymal cells from the capillary fraction, immunohistochemical analysis showed that claudin-11 signals were only seen in the capillaries (not oligodendrocytes) in human brain sections, as shown in Fig. 2d, so the protein expression level of claudin-11 in brain capillary endothelial cells may be greater in human than rat. In addition, the signal of claudin-11 was also predominantly observed in the capillaries in human spinal cord sections (Fig. 2d), whereas in mouse spinal cord sections, it was observed not only in the capillaries but also in oligodendrocytes (Fig. 1c). Therefore, spinal cord capillary endothelial cells may also have a greater protein expression level of claudin-11 in human than rodent. However, the numbers of donors used in the present study was limited. Although our previous quantitative proteomics study has shown that the inter-individual differences in the protein expression levels for most of the membrane proteins in the isolated human brain capillaries were within approximately 2-fold range [18], further quantification of claudin-11 using more human donors

Fig. 5 Cis and trans binding patterns of claudin-11 and claudin-5 in tight junctions. **a** Claudin-11-transfected HEK293 cells were cultured and stained with antibodies against claudin-11 (green). Nuclei were stained with PI (red). Scale bar, 25 μm. High-magnification images (i and ii) are shown in the *right side*, and arrowheads indicate plasma membrane locations where there is no neighboring cell. The binding pattern of claudin-11 (green strand) is illustrated using two claudin-11-transfected cells (green color cells). **b** Claudin-5-transfected HEK293 cells were cultured and stained with antibodies against claudin-5 (green). Nuclei were stained with PI (red). Scale bar, 25 μm. High-magnification images (i and ii) are shown on the *right side*, and arrowheads indicate plasma membrane locations where there is no neighboring cell. The binding pattern of claudin-5 (red strand) is illustrated using two claudin-5-transfected cells (red-colored cells). **c** Claudin-11-transfected HEK293 cells and claudin-5-transfected HEK293 cells were co-cultured and co-stained with antibodies against claudin-11 (green) and claudin-5 (red). Scale bar, 25 μm. High-magnification image (i) is shown on the *right side*, and arrowheads indicate plasma membrane locations where claudin-11-transfected and claudin-5-transfected HEK293 cells are adjoining. The binding pattern of claudin-5 (red strand) and claudin-11 (green strand) is illustrated using one claudin-5-transfected cell (red color cell) and one claudin-11-transfected cell (green color cell). **d** HEK293 cells double-transfected with claudin-11 and claudin-5 were cultured and co-stained with antibodies against claudin-11 (green) and claudin-5 (red). Scale bar, 25 μm. High-magnification images (i and ii) are shown on the *right side*, and arrowheads indicate the plasma membrane locations where there are neighboring cells (ii) and no neighboring cell (i). The binding pattern of claudin-5 (red strand) and claudin-11 (green strand) is illustrated using two double-transfected cells (yellow color cells). **a–d** Circle and cross represent that the binding in the indicated direction (cis or trans) is suggested and not suggested based on the immunostaining data, respectively. **e** Two possible models for cis and trans binding of claudin-11 and claudin-5 in cells expressing both (such as brain and spinal cord capillary endothelial cells), based on the results in **a–d**. Claudin-11 and claudin-5 strands are illustrated in green and red, respectively
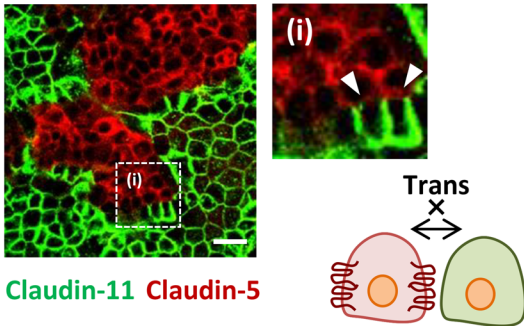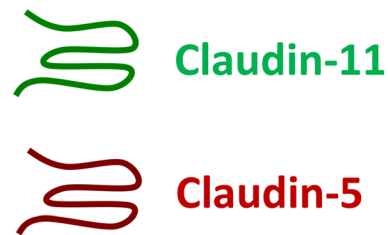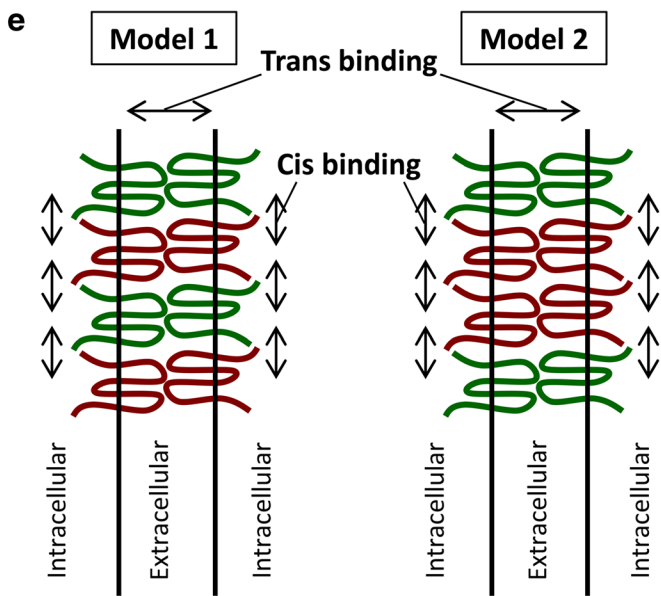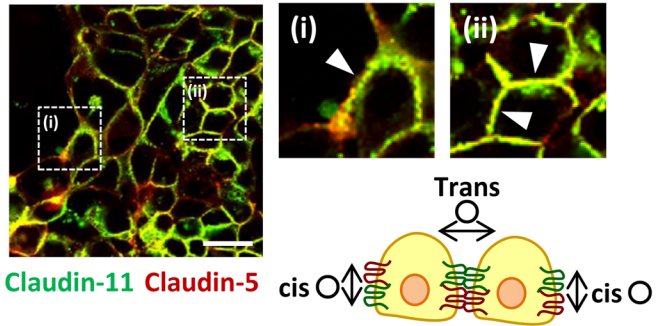
a Monoculture of claudin-11 expressing cells

b Monoculture of claudin-5 expressing cells
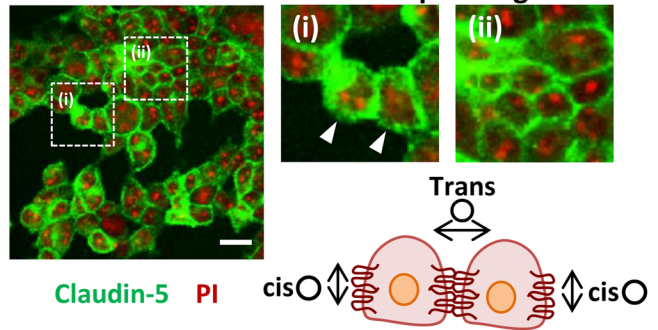
c Co-culture of claudin-11 and 5 expressing cells

**d Monoculture of claudin-11 and 5 co-expressing cells**

e

would be needed in future to determine the average and variance of claudin-11 expression level at the human BBB and BSCB, and carefully discuss the species difference in the claudin-11 level.
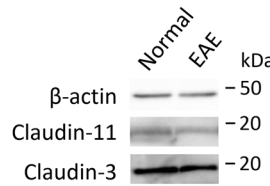
The results of immunohistochemical co-staining indicate that the claudin-11 and claudin-5 co-exist in same endothelial cell, because the claudin-11 signal was completely overlapped with the claudin-5 signal in brain and spinal cord capillaries (Figs. 1c and 2d). Therefore, it is also important to understand their relative contributions to tight-junction formation in the

same endothelial cell. Based on the result of the siRNA knockdown experiment in the hCMEC/D3 cell, we calculated the extent of contribution of claudin-11 or claudin-5 per 1 mol ("single-molecule activity" in Table 1). Then, we multiplied it by the absolute protein expression level in the human isolated brain capillaries in order to calculate the contribution at the human BBB ("Activity at the human blood-brain barrier" in Table 1). The contributions of claudin-11 and claudin-5 were almost equal. "The contribution of claudin-11 or claudin-5 per 1 mole (single-molecule activity)" described
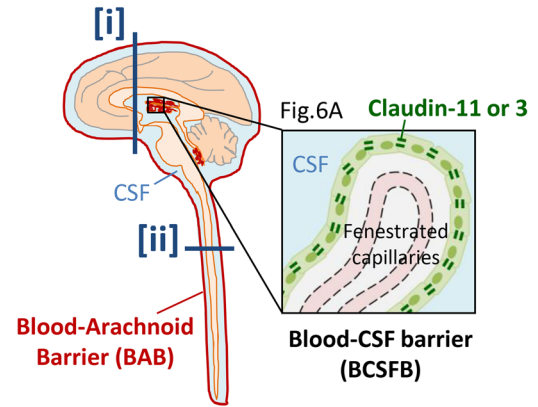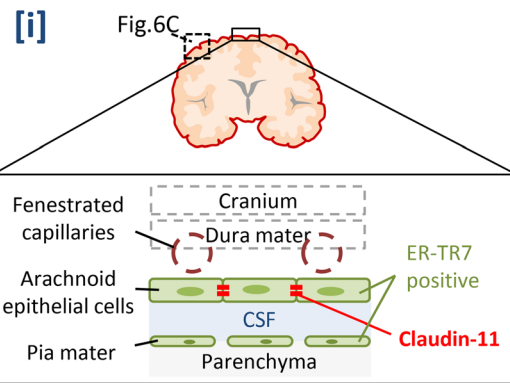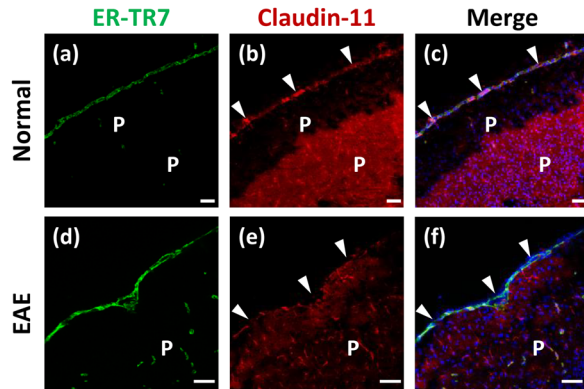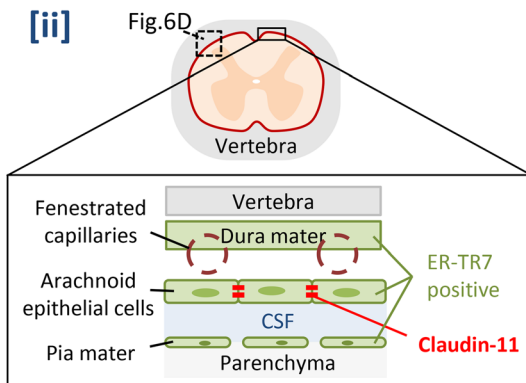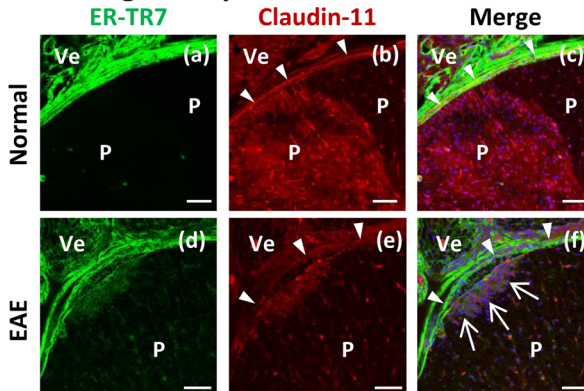
a Choroid plexus
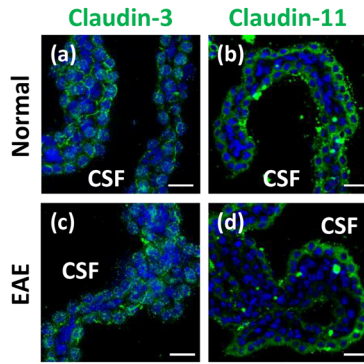
b Choroid plexus (Western blot)

c Meninges in brain

d Meninges in spinal cord

e Illustration of BCSFB and BAB

f Knockdown of claudin-11 protein by siRNA in TR-CSFB cell monolayer
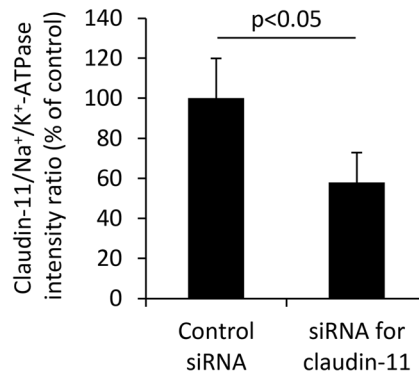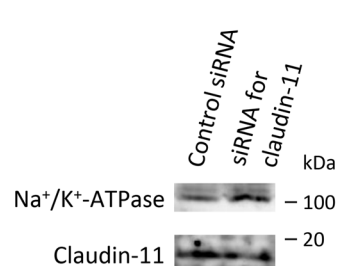
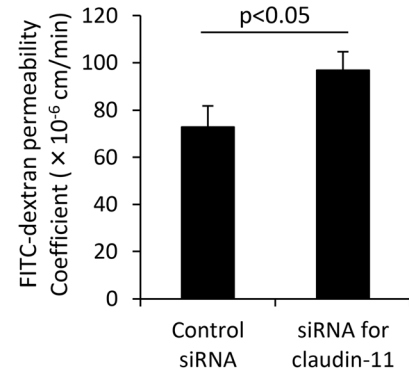**g** Paracellular permeability in TR-CSFB cell monolayer

◄ **Fig. 6** Protein expression of claudin-11 at the central nervous system epithelial barriers in EAE mouse, and the influence of claudin-11 downregulation on the barrier integrity of an epithelial cell monolayer. EAE mice with a clinical score of 3 to 3.5 (limp tail and complete paralysis of hind legs) were used for immunohistochemistry. **a** Brains excised from normal and EAE mice were frozen with dry ice and sliced into 20-μm sections with a cryostat. The slices including choroid plexus were fixed with cold acetone and stained with antibodies against claudin-11 (green; *b, d*) or claudin-3 (green; *a, c*). Nuclei were stained with DAPI (blue). Scale bar, 25 μm. *CSF* cerebrospinal fluid. **b** Whole-tissue lysates of the pooled choroid plexuses of two normal mice or two EAE mice were subjected to SDS-PAGE, followed by western blot analysis using anti-claudin-11, anti-claudin-3, and anti-β-actin antibodies. Molecular mass in kilo Daltons is shown on the *right*. **c** The brains excised from normal and EAE mice (cranium and dura mater were removed) were frozen with dry ice and sliced into 20-μm sections with a cryostat. The slices were fixed with cold acetone and co-stained with antibodies against ER-TR7 (a meningeal cell marker) (green; *a, d, c, f*) and claudin-11 (red; *b, e, c, f*). Nuclei were stained with DAPI (blue in merged images; *c, f*). Scale bar, 75 μm. Arrowheads indicate the meninges, where the claudin-11 signal appears in normal mice and is lost in EAE mice. *P* parenchymal tissue. **d** The upper thoracic backbone (including the upper thoracic spinal cord) was excised from normal and EAE mice (vertebra and dura mater were not removed), frozen with dry ice, and sliced into 20-μm sections with a cryostat. The slices were fixed with cold acetone and co-stained with antibodies against ER-TR7 (green; *a, d, c, f*) and claudin-11 (red; *b, e, c, f*). Nuclei were stained with DAPI (blue in merged images; *c, f*). Scale bar, 75 μm. Arrowheads indicate the meninges, where the claudin-11 signal appears in normal mice and is lost in the EAE mice. Arrows indicate DAPI (blue) signals, suggesting the presence of many cells. *P* parenchymal tissue, *Ve* vertebra. **e** The structures of the choroid plexus including the BCSFB and the meninges including the BAB are illustrated. In the choroid plexus, claudin-3 and claudin-11 are expressed in epithelial cells forming the tight junctions (BCSFB). The brain and spinal cord sections used in **c, d** were prepared by slicing the tissues along with the blue lines (i) and (ii), respectively. The structures of the meninges in these brain and spinal cord sections are illustrated. The boxes marked with dotted lines (**c, d**) represent almost the same positions as the pictures in **c, d**, respectively. In the case of the brain meninges, the cranium and dura mater were removed before the immunostaining, and so these are illustrated with dotted lines. Meninges consist of dura mater, arachnoid epithelial cells, and pia mater, which are all ER-TR7-positive and are shown in green. In meninges, only arachnoid epithelial cells form tight junctions, so it is considered that the signals of claudin-11 (red thin lines) overlapping with ER-TR7 signals in the meninges in **c, d** represent claudin-11 in arachnoid epithelial cells. **f** TR-CSFB cells were treated with 50-nM negative control siRNA or claudin-11 siRNA for 6 h and cultured in medium without siRNA for 18 h. TR-CSFB cells were cultured for 7 days, and the plasma membrane fraction was prepared with a Minute Plasma Membrane Protein Isolation Kit. The sample was subjected to SDS-PAGE, followed by western blot analysis using anti-claudin-11 and anti-Na$^+$/K$^+$-ATPase antibodies. Molecular mass in kilo Daltons is shown on the *right*. The band intensity was calculated with ImageJ software and normalized over the area selected. The band intensity of claudin-11 was normalized with respect to Na$^+$/K$^+$-ATPase intensity. The band intensity ratio (claudin-11/ Na$^+$/K$^+$-ATPase) under the control siRNA condition was normalized to 100%. $p < 0.05$, an unpaired two-tailed Student's *t* test was used to determine the significance of differences between two groups. The data represent mean ± SD ($n = 3$). **g** TR-CSFB cells were treated with siRNA, cultured in 6-well Transwell plates for 7 days under the same experimental conditions as in the case of the western blot experiment, and then used for FITC-dextran permeability analysis. After removal of the medium, 1 mg/mL FITC-dextran (70 kDa) solution (1.5 mL) was added to the Transwell insert. The concentration of FITC-dextran in the receiver well was measured at 15, 30, and 45 min. The permeability coefficient was calculated as described in the "Materials and Methods" section. $p < 0.05$, an unpaired two-tailed Student's *t* test was used to determine the significance of differences between two groups. The data represent the mean ± SD ($n = 3$)

above represents how much the permeability of the membrane-impermeable FITC-dextran across the hCMEC/D3 cell monolayer increases when the protein expression level of each claudin decreases by 1 mol. Therefore, "the contribution at the human BBB (Activity at the human blood-brain barrier)" described above represents how strongly each claudin at the human BBB contributes to the limitation of permeation of membrane-impermeable substances across the human BBB.

It appears that claudin-5 plays an important role in stabilizing claudin-11 expression, because claudin-11 was significantly downregulated by the knockdown of claudin-5 (Fig. 4b). To verify this, we examined the interaction pattern of these two molecules. Claudin-11 was localized at all the plasma membranes when both claudins were co-expressed in the same cells (Fig. 5d), while no signal of claudin-11 was observed at the plasma membrane in locations where there is no neighboring cell when only claudin-11 is expressed (Fig. 5a). It has been reported that claudin-4 and claudin-8 or claudin-16 and claudin-19 are stabilized on the membrane via cis binding with each other in renal epithelial cells [24, 25]. Similarly, our results suggest that cis binding of claudin-11 could be destabilized by the knockdown of claudin-5. In contrast, claudin-5 appears to be stabilized on the plasma membrane via both cis and

trans bindings (Fig. 5b). This is consistent with the observation that knockdown of claudin-11 in the hCMEC/D3 cell monolayer did not significantly influence claudin-5 expression (Fig. 4b). These facts, which the expression of claudin-11 depended on that of claudin-5 but the expression of claudin-5 did not depend on that of claudin-11, may indicate that the claudin-5 functions as an upstream regulator of the expression of claudin-11. Therefore, claudin-5 may substantially contribute to the tight junction formation more strongly than claudin-11 at the human BBB, although the individual contribution of claudin-11 and claudin-5 was estimated to be almost equal above. Furthermore, regarding trans binding, claudin-11 can bind to claudin-11, whereas claudin-11 and claudin-5 cannot bind with each other (Fig. 5a, c). Overall, we propose that claudin-11 and claudin-5 interact in the manner shown in model 1 or 2 (Fig. 5e) to form tight junctions.

Our previous study raised the possibility that claudin-11, unlike claudin-5, plays an important role in forming the CNS epithelial barriers as well as the CNS endothelial barriers, because the absolute protein expression level of claudin-11 was higher than those of other tight-junction proteins in the human choroid plexus [26]. Thus, we investigated the importance of claudin-11 at the BCSFB and BAB. As shown in Fig. 6, claudin-11 was observed not only

at the plasma membrane of choroid plexus epithelial cell but also in the brain and spinal cord meninges, because the claudin-11 signals overlapped with the signals of ER-TR7, which is a marker of dura (thick), arachnoid (thin), and pia (thin) mater. Among the dura, arachnoid, and pia mater, only arachnoid epithelial cell forms tight junctions [27]. Therefore, claudin-11 is considered to be expressed on arachnoid epithelial cells. The knockdown experiment with TR-CSFB cells suggested that claudin-11 contributes to the formation of CNS epithelial barriers (Fig. 6f, g), although we could not obtain arachnoid epithelial cell monolayers. In EAE mice, the protein expression level of claudin-11 was significantly decreased at the arachnoid mater of the brain and spinal cord (Fig. 6c, d). However, it was not significantly decreased in the choroid plexus, as was also the case for claudin-3, which is an important claudin subtype at the BCSFB (Fig. 6a, b). Approximately 80% of the CSF volume exist in the subarachnoid space, which faces the BAB, not the BCSFB [28]. The invasion of lymphocytes into the CSF in MS occurs via the leptomeninges of the spinal cord to a greater extent than via the choroid plexus [16]. This is consistent with the downregulation of claudin-11 at the BAB, but not the BCSFB, in the EAE mice, suggesting that claudin-11 could be a major claudin subtype in the CNS epithelial barrier, and its downregulation in MS may permit the invasion of lymphocytes into the CSF from circulating blood via the meninges.

The extent of disability in MS is better correlated with atrophy of the spinal cord than that of the brain [14], and this suggests that the spinal cord is more likely to be damaged. In EAE mice, the absolute protein expression level of claudin-11 was 2.46-fold smaller in the capillaries of the spinal cord than in those of the brain (Fig. 3d). The decrease of claudin-11 expression in the MS patient was greater in the spinal cord (48.4%) than in the brain (39.4%) (Fig. 3f, h). In the low-magnification immunostaining pictures of both EAE mice and the MS patient, the signals of claudin-11 in the spinal cord capillaries were broadly weakened (Supplemental Fig. 4). Also, in locations where claudin-11 expression was downregulated in the spinal cord arachnoid mater, invasion of T lymphocytes into parenchyma was observed by immunostaining of CD3e, a T lymphocyte marker (Fig. 6d and Supplemental Figs. 5 and 6). The greater downregulation of claudin-11 in the spinal cord region could explain the more significant barrier breakdown and atrophy in spinal cord than brain.

The findings in female EAE mice and the male MS patient suggest that claudin-11 expression may be downregulated in both males and females with MS (Fig. 3). DHT suppressed the loss of claudin-11 from the plasma membrane of hCMEC/D3 cell exposed to EAE serum (Fig. 4a). Also, in the normal human brain sections, the signal intensities of claudin-11 were not significantly different between males and females (Fig. 2d). These results suggest that claudin-11 expression level is not induced by androgen, at least under normal conditions. On the other hand, testosterone suppresses the degradation of tight-junction molecules induced by TGF-β2 and TNF-α in Sertoli cells and stabilizes them on the membrane [29, 30]. This supports the idea that androgen maintains the expression and membrane localization of claudin-11 by suppressing inflammatory cytokine-induced degradation in MS, rather than by increasing the transcription of claudin-11. Because the hCMEC/D3 cell line is derived from a female [17], the present results (Fig. 4a) may imply that androgen also plays a role in maintaining claudin-11 expression in females. This would be consistent with the observation that female MS patients with a lower blood testosterone level exhibit greater disruption of CNS barriers [11]. However, one potential issue is that the human brain and spinal cord sections used in the present study were only derived from a male MS patient but not female ones. Further study would be needed in future to generalize the role of claudin-11 to female MS patients.

Claudin-5 expression is downregulated in the brain capillaries in MS [31], and this might lead to downregulation of claudin-11 expression in MS because the binding of claudin-11 in the cis direction is destabilized by the loss of claudin-5. Our comprehensive proteomic analysis did not detect any claudin subtypes other than claudin-5 and claudin-11 (Fig. 1a). Therefore, the simultaneous downregulation of claudin-5 and claudin-11 in MS could account for the significant disruption of CNS barriers. However, claudin-5 knockout mice did not show altered permeability of > 800-Da molecules compared to wild-type mice [32], even though claudin-11 expression is considered to be decreased as well. Other proteins such as occludin and ZO-1 also support the formation of tight junction, but do not contribute substantially to the barrier integrity. Therefore, it is possible that some other unidentified molecule is also involved in tight-junction integrity. On the other hand, we found that in a hCMEC/D3 cell monolayer, the knockdown of claudin-5 downregulated claudin-11 expression and increased the permeability of 70 kDa dextran (Fig. 4b, c). Further work will be needed to establish the reason for the difference between the results in mice and hCMEC/D3 cells, although it should be noted that barrier integrity of a hCMEC/D3 cell monolayer is weak compared to that of in vivo tight junctions [17].

In the present study, the in vitro hCMEC/D3 and TR-CSFB cell monolayers were used to show that the claudin-11 is involved in the integrities of CNS endothelial and epithelial barriers, respectively. However, it is necessary to conduct the in vivo permeability experiment using the claudin-11 knockout mice in order to demonstrate the in vivo contribution of claudin-11 at the CNS barriers. Furthermore, it would be important to examine whether the claudin-11 knockout mice is more likely to induce the EAE than wild-type mice in order to properly clarify the involvement of claudin-11 in the onset and progression of MS.

A critical issue in the present study was that the sample size is small, although the downregulation of claudin-11 protein expression at the CNS barriers was demonstrated both in EAE mice and MS patient. Three EAE mice were used for each experiment because we were stably able to generate the EAE mice with the clinical score more than 3.0. To properly conclude that the claudin-11 expression level is downregulated in the MS, further study using more mice and MS patient samples would be needed in future. It is also important to clarify the differences in the extent of downregulation of claudin-11 level among the different regions of brain and spinal cord or the different disease state of MS, in order to clarify how general the preliminary findings in the present study are in the MS.

In conclusion, our present results demonstrate firstly that the protein expression level of claudin-11 is significantly downregulated at the BBB, BSCB, and BAB, but not BCSFB, in MS, and secondly that downregulation of claudin-11 expression decreases the integrity of the CNS endothelial and epithelial barriers. These findings advance our understanding of the molecular mechanisms of CNS barrier breakdown in MS, and indicate that prevention of claudin-11 downregulation may be a promising strategy for the treatment of MS. However, the present study is a preliminary one because the sample size was small. Further study using more samples would be needed to properly understand the pathophysiological role of claudin-11 at the CNS barriers in the MS in detail.

Compliance with Ethical Standards

Conflicts of Interest Tetsuya Terasaki and Sumio Ohtsuki are full professors at Tohoku University and Kumamoto University, and are also directors of Proteomedix Frontiers Co., Ltd. This study was not supported by Proteomedix Frontiers Co., Ltd., and their positions at Proteomedix Frontiers Co., Ltd., did not influence the design of the study, the collection of data, the analysis or interpretation of data, the decision to submit the manuscript for publication, or writing of the manuscript. There were no financial conflicts. The other authors declare no competing interests.

References

1. Kermode AG, Thompson AJ, Tofts P, MacManus DG, Kendall BE, Kingsley DP, Moseley IF, Rudge P et al (1990) Breakdown of the blood-brain barrier precedes symptoms and other MRI signs of new lesions in multiple sclerosis. Pathogenetic and clinical implications. Brain 113(Pt 5):1477–1489

2. Errede M, Girolamo F, Ferrara G, Strippoli M, Morando S, Boldrin V, Rizzi M, Uccelli A et al (2012) Blood-brain barrier alterations in the cerebral cortex in experimental autoimmune encephalomyelitis. J Neuropathol Exp Neurol 71(10):840–854. https://doi.org/10.1097/NEN.0b013e31826ac110

3. Kooij G, Kopplin K, Blasig R, Stuiver M, Koning N, Goverse G, van der Pol SM, van Het Hof B et al (2014) Disturbed function of the blood-cerebrospinal fluid barrier aggravates neuro-inflammation. Acta Neuropathol 128(2):267–277. https://doi.org/10.1007/s00401-013-1227-1

4. Hellani A, Ji J, Mauduit C, Deschildre C, Tabone E, Benahmed M (2000) Developmental and hormonal regulation of the expression of oligodendrocyte-specific protein/claudin 11 in mouse testis. Endocrinology 141(8):3012–3019. https://doi.org/10.1210/endo.141.8.7625

5. Tiwari-Woodruff SK, Buznikov AG, Vu TQ, Micevych PE, Chen K, Kornblum HI, Bronstein JM (2001) OSP/claudin-11 forms a complex with a novel member of the tetraspanin super family and beta1 integrin and regulates proliferation and migration of oligodendrocytes. J Cell Biol 153(2):295–305

6. Brochner CB, Holst CB, Mollgard K (2015) Outer brain barriers in rat and human development. Front Neurosci 9:75. https://doi.org/10.3389/fnins.2015.00075

7. Romanitan MO, Popescu BO, Spulber S, Bajenaru O, Popescu LM, Winblad B, Bogdanovic N (2010) Altered expression of claudin family proteins in Alzheimer's disease and vascular dementia brains. J Cell Mol Med 14(5):1088–1100. https://doi.org/10.1111/j.1582-4934.2009.00999.x

8. Wolburg H, Wolburg-Buchholz K, Liebner S, Engelhardt B (2001) Claudin-1, claudin-2 and claudin-11 are present in tight junctions of choroid plexus epithelium of the mouse. Neurosci Lett 307(2):77–80

9. Florin A, Maire M, Bozec A, Hellani A, Chater S, Bars R, Chuzel F, Benahmed M (2005) Androgens and postmeiotic germ cells regulate claudin-11 expression in rat Sertoli cells. Endocrinology 146(3):1532–1540. https://doi.org/10.1210/en.2004-0834

10. Kaitu'u-Lino TJ, Sluka P, Foo CF, Stanton PG (2007) Claudin-11 expression and localisation is regulated by androgens in rat Sertoli cells in vitro. Reproduction 133(6):1169–1179. https://doi.org/10.1530/REP-06-0385

11. Tomassini V, Onesti E, Mainero C, Giugni E, Paolillo A, Salvetti M, Nicoletti F, Pozzilli C (2005) Sex hormones modulate brain damage in multiple sclerosis: MRI evidence. J Neurol Neurosurg Psychiatry 76(2):272–275. https://doi.org/10.1136/jnnp.2003.033324

12. Zhu ML, Bakhru P, Conley B, Nelson JS, Free M, Martin A, Starmer J, Wilson EM et al (2016) Sex bias in CNS autoimmune disease mediated by androgen control of autoimmune regulator. Nat Commun 7:11350. https://doi.org/10.1038/ncomms11350

13. Prockop LD, Naidu KA, Binard JE, Ransohoff J (1995) Selective permeability of [3H]-D-mannitol and [14C]-carboxyl-inulin across the blood-brain barrier and blood-spinal cord barrier in the rabbit. J Spinal Cord Med 18(4):221–226

14. Schlaeger R, Papinutto N, Zhu AH, Lobach IV, Bevan CJ, Bucci M, Castellano A, Gelfand JM et al (2015) Association between thoracic spinal cord gray matter atrophy and disability in multiple sclerosis. JAMA Neurol 72(8):897–904. https://doi.org/10.1001/jamaneurol.2015.0993

15. Winkler EA, Sengillo JD, Bell RD, Wang J, Zlokovic BV (2012) Blood-spinal cord barrier pericyte reductions contribute to increased capillary permeability. J Cereb Blood Flow Metab 32(10):1841–1852. https://doi.org/10.1038/jcbfm.2012.113

16. Schlager C, Korner H, Krueger M, Vidoli S, Haberl M, Mielke D, Brylla E, Issekutz T et al (2016) Effector T-cell trafficking between

the leptomeninges and the cerebrospinal fluid. Nature 530(7590): 349–353. https://doi.org/10.1038/nature16939

17. Weksler BB, Subileau EA, Perriere N, Charneau P, Holloway K, Leveque M, Tricoire-Leignel H, Nicotra A et al (2005) Blood-brain barrier-specific properties of a human adult brain endothelial cell line. FASEB J 19(13):1872–1874. https://doi.org/10.1096/fj.04-3458fje

18. Uchida Y, Ohtsuki S, Katsukura Y, Ikeda C, Suzuki T, Kamiie J, Terasaki T (2011) Quantitative targeted absolute proteomics of human blood-brain barrier transporters and receptors. J Neurochem 117(2):333–345

19. Hoshi Y, Uchida Y, Tachikawa M, Inoue T, Ohtsuki S, Terasaki T (2013) Quantitative atlas of blood-brain barrier transporters, receptors, and tight junction proteins in rats and common marmoset. J Pharm Sci 102(9):3343–3355. https://doi.org/10.1002/jps.23575

20. Kamiie J, Ohtsuki S, Iwase R, Ohmine K, Katsukura Y, Yanai K, Sekine Y, Uchida Y et al (2008) Quantitative atlas of membrane transporter proteins: development and application of a highly sensitive simultaneous LC/MS/MS method combined with novel in-silico peptide selection criteria. Pharm Res 25(6):1469–1483

21. Uchida Y, Ohtsuki S, Kamiie J, Terasaki T (2011) Blood-brain barrier (BBB) pharmacoproteomics: reconstruction of in vivo brain distribution of 11 P-glycoprotein substrates based on the BBB transporter protein concentration, in vitro intrinsic transport activity, and unbound fraction in plasma and brain in mice. J Pharmacol Exp Ther 339(2):579–588. https://doi.org/10.1124/jpet.111.184200

22. Morgan L, Shah B, Rivers LE, Barden L, Groom AJ, Chung R, Higazi D, Desmond H et al (2007) Inflammation and dephosphorylation of the tight junction protein occludin in an experimental model of multiple sclerosis. Neuroscience 147(3):664–673. https://doi.org/10.1016/j.neuroscience.2007.04.051

23. Ohtsuki S, Yamaguchi H, Katsukura Y, Asashima T, Terasaki T (2008) mRNA expression levels of tight junction protein genes in mouse brain capillary endothelial cells highly purified by magnetic cell sorting. J Neurochem 104(1):147–154. https://doi.org/10.1111/j.1471-4159.2007.05008.x

24. Gong Y, Renigunta V, Zhou Y, Sunq A, Wang J, Yang J, Renigunta A, Baker LA et al (2015) Biochemical and biophysical analyses of tight junction permeability made of claudin-16 and claudin-19

25. Hou J, Renigunta A, Yang J, Waldegger S (2010) Claudin-4 forms paracellular chloride channel in the kidney and requires claudin-8 for tight junction localization. Proc Natl Acad Sci U S A 107(42): 18010–18015. https://doi.org/10.1073/pnas.1009399107

26. Uchida Y, Zhang Z, Tachikawa M, Terasaki T (2015) Quantitative targeted absolute proteomics of rat blood-cerebrospinal fluid barrier transporters: comparison with a human specimen. J Neurochem 134(6):1104–1115. https://doi.org/10.1111/jnc.13147

27. Kolias AG, Chari A, Santarius T, Hutchinson PJ (2014) Chronic subdural haematoma: modern management and emerging therapies. Nat Rev Neurol 10(10):570–578. https://doi.org/10.1038/nrneurol.2014.163

28. Thorne RG (2014) Primer on central nervous system structure/function and the vasculature, ventricular system, and fluids of the brai. In: Hammarlund-Udenaes M, de Lange E, Thorne RG (eds) Drug delivery to the brain - physiological concepts, methodologies and approaches. Springer, pp. 685–707

29. Lui WY, Lee WM (2009) Molecular mechanisms by which hormones and cytokines regulate cell junction dynamics in the testis. J Mol Endocrinol 43(2):43–51. https://doi.org/10.1677/JME-08-0174

30. Yan HH, Mruk DD, Lee WM, Cheng CY (2008) Blood-testis barrier dynamics are regulated by testosterone and cytokines via their differential effects on the kinetics of protein endocytosis and recycling in Sertoli cells. FASEB J 22(6):1945–1959. https://doi.org/10.1096/fj.06-070342

31. Lanz TV, Becker S, Osswald M, Bittner S, Schuhmann MK, Opitz CA, Gaikwad S, Wiestler B et al (2013) Protein kinase Cbeta as a therapeutic target stabilizing blood-brain barrier disruption in experimental autoimmune encephalomyelitis. Proc Natl Acad Sci U S A 110(36):14735–14740. https://doi.org/10.1073/pnas.1302569110

32. Nitta T, Hata M, Gotoh S, Seo Y, Sasaki H, Hashimoto N, Furuse M, Tsukita S (2003) Size-selective loosening of the blood-brain barrier in claudin-5-deficient mice. J Cell Biol 161(3):653–660. https://doi.org/10.1083/jcb.200302070